Theor. Appl. Climatol. 92, 1–14 (2008)
DOI 10.1007/s00704-007-0315-3
Printed in The Netherlands

Theoretical
and Applied
Climatology

[1] Faculty of Science, Bindura University of Science Education, Bindura, Zimbabwe
[2] Faculty of Environmental Science, National University of Lesotho, Lesotho

The superior influence of Darwin Sea level pressure anomalies over ENSO as a simple drought predictor for Southern Africa

D. Manatsa[1], **W. Chingombe**[1], **H. Matsikwa**[1], and **C. H. Matarira**[2]

With 7 Figures

Received April 21, 2006; revised December 14, 2006; accepted March 7, 2007
Published online October 4, 2007

Summary

The dominant climatic mode responsible for seasonal rainfall variability across central southern Africa has been well-established as ENSO. Hence, the El Niño signal of the equatorial Pacific has been used extensively to predict droughts in this sub-region. Although this paper acknowledges that El Niño influences rainfall deficits over eastern southern Africa, an earlier signal of extreme positive sea level pressure (SLP) anomalies at Darwin for the averaged March to June period (MAMJ Darwin) has proved to have a superior remote connection to droughts in the sub-region. Simple linear statistical tools including composite techniques and correlation methods have been employed on century long data sets (1901–2000) to identify the emerging paramount connection between MAMJ Darwin SLP anomalies and southern African rainfall.

Both MAMJ Darwin SLP anomalies and the Zimbabwe seasonal rainfall time series are significantly correlated (above the 95% significant level) with sea surface temperature anomalies. These represent the Indian Ocean Dipole mode in the tropical Indian Ocean and ENSO in the tropical Pacific for the averaged September to December period. 'Pure' MAMJ Darwin (that occur in the absence of El Niño in the Pacific) coincide with droughts more significantly (83% hit rate) than 'pure' El Niño events (not preceded by a high MAMJ Darwin) (38% hit rate). Co-occurrences (MAMJ Darwin preceded by El Niño) do not only have the highest hit rate of 93% but subsequent droughts are noticeably more severe. The 'pure' El Niños however, are not only poorly related to Zimbabwe seasonal rainfall deficits, but are apparently not connected to extreme droughts of the 20th century. Thus, MAMJ Darwin is a good simple predictor of droughts associated with or without ENSO in the Pacific. The high prediction skill of these results, especially the inherent longer lead-time than ENSO, makes MAMJ Darwin SLP anomalies an ideal additional input candidate for sub-regional drought monitoring and forecasting schemes. In this way, drought early warning and disaster preparedness activities can be enhanced over the sub-region.

1. Introduction

1.1 Drought disaster in Southern Africa

Southern Africa, which is largely semi-arid, is characterised by high seasonal rainfall variability (Rasmusson and Eugene, 1987) and as such drought periods occur with relatively high frequency and severity. Because of the low socio-economic status of the sub-region, droughts, easily become natural disasters. The main problem is that, although drought is of recognisable recurrence, regional seasonal weather forecasts still present low levels of confidence and accuracy. Agriculture, which is predominantly rain-fed, forms the backbone of the economy of the region. Failure of the rainfall regime is more likely to cause serious disruption to the natural as well as to agricultural ecosystems and lead to a corresponding failure of many sectors of the economy.

This condition would readily translate into untold suffering and even death among the already vulnerable, predominantly poor rural populations of the region (e.g. World Bank, 2006). For example, from 1982 to 1984, maize yields south of the Zambezi valley declined to 10% of historical values and 80% of livestock perished (Makarau, 1995). In the 1992 drought, water availability became critical as 90% of small dams dried up in Botswana, South Africa, Zimbabwe and Namibia (Jury and Mwafulirwa, 2002).

A reduction in drought-related impacts could be achieved, with the provision of reliable drought predictions, with adequate lead-times. Forecasting droughts in this sub-region has not been reliable in recent years, a result of the challenges of developing early warning skills appropriate to the climatic and agricultural conditions prevailing in the area (Cane et al., 1994; Waylen and Henworth, 1996; Phillips et al., 1998). Thus, in this paper we attempt to address the drought forecast skill as well as the lead-time constraint by proposing an alternative simple drought predictor for southern Africa. In this way we hope the related adverse effects of these climate fluctuations might be mitigated.

1.2 El Niño Southern Oscillation (ENSO)

Important progress is being made in relation to the possibilities of using the El Niño Southern Oscillation (ENSO) in seasonal prediction. ENSO events in the equatorial Pacific have long been believed to be the major mechanism for seasonal rainfall variation of southern Africa (Ropelewski and Halpert, 1987; Matarira, 1990; Shinod and Kawamura, 1996; Rocha and Simmonds, 1997). Hence, recurring droughts are attributed mostly to the influence of El Niño. As such, recent developments in seasonal rainfall forecasting techniques in southern Africa have come to rely heavily on ENSO related predictability (Washington et al., 2003). From 1998, the Southern African Developing Countries (SADC) Drought Monitoring Center (DMC Harare), in conjunction with the International Research Institute (IRI, USA), have organized annual Southern Africa Regional Climate Outlook Forums (SARCOF) in order to develop seasonal forecasts using ENSO indices as the primary predictors.

It is important to note that the timely and appropriate implementation of policies and measures to prevent a drought from becoming a disaster largely depends on the lead-time. This crucial factor is not adequately provided by ENSO indices, as they inherit a lead-time constraint. They can only become useful with considerable skill for the users towards the beginning of the season. In the case of agriculture several months lead-time is essential to enable farmers to make decisions regarding the altering of crop and agricultural systems in order to cope with forecasted droughts (Paulo et al., 2005).

Relying on ENSO indices alone for sub-regional drought prediction also presents additional problems related to forecast skill. In previous years, ENSO events have failed to explain all extreme rainfall events (Fauchereau et al., 2003; Rouault and Richard, 2005). For example, in Zimbabwe, only three of the seven extreme droughts of the 20^{th} century occurred during El Niño. The most intense El Niño of the century (1997/98) was related to a small deficit in total seasonal rainfall. The strong La Niña of 1967/68, which is supposed to present an influence opposite to that of El Niño, was linked to a very severe drought. This may indicate that the influence of ENSO events has been overrated, especially as a major cause of the sub-region's droughts. Hence, it is appropriate to focus attention on identifying and investigating other plausible climate forcing factors.

1.3 Indian Ocean Dipole (IOD) mode

Apart from the global scale ENSO influence, many authors have pointed out that inter-annual rainfall variability over large parts of southern Africa is linked to sea surface temperature (SST) anomalies over the surrounding Indian Ocean (IO) (Walker, 1990; Reason, 1999; Reason and Mulenga, 1999). They link the warming of the western equatorial IO to dry conditions over southern Africa. This area also coincides with the western pole of a phenomenon that is believed to occur in the IO. This phenomenon is referred to as the Indian Ocean Dipole (IOD) mode, which is believed to be one of the major ocean-atmosphere coupled phenomena in the tropical IO (Saji et al., 1999; Webster et al., 1999; Yamagata et al., 2002; Behera et al., 2005). The IOD is an anomalous periodic climate mode that occurs interannually in the tropical parts of the IO. It involves radical changes in standard ocean-atmosphere conditions and/or interactions between the east-

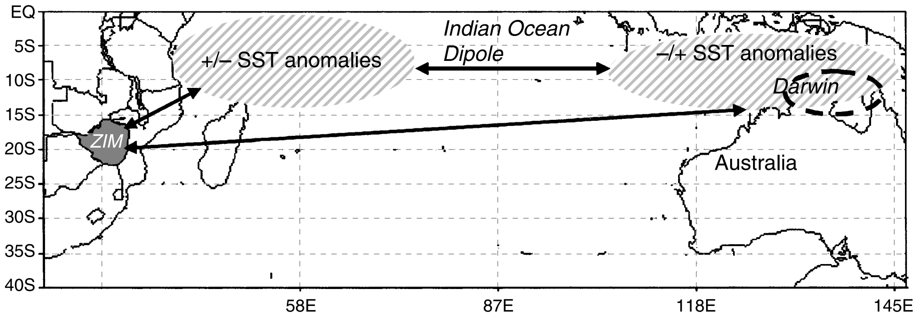

Fig. 1. Location map of the study area. Map of the Indian Ocean indicates the region of the Zimbabwe seasonal SPI values (Zim SPI, Standardised Precipitation Index), the Darwin Sea level Pressure anomalies and the western Tropical Indian Ocean SST sector. The shaded region shows the major areas used to define the IOD

ern and western regions, with a peak period from September to November (Yamagata et al., 2003).

The IOD mode appears to have a complicated relationship with ENSO, occurring at times of ENSO extremes and at other times when the Pacific is not anomalous (Clark et al., 2000; Reason et al., 2000; Saji et al., 1999; Webster et al., 1999). Its complexity together with its short research history, has led some researchers such as Baquero-Bernal and Latif (2002) and Allan et al. (2001) to question its existence as well as its independence from ENSO. Chambers et al. (1999) related this IO SST dipole as an extension of the Indo-Australian node of the Southern Oscillation (SO) component of ENSO into the Indian Ocean. However, the physical existence of the IOD has been amply demonstrated by showing that the IOD is an internal coupled mode in the Indian Ocean, which at times co-occurs with the ENSO in the Pacific (Saji et al., 1999; Webster et al., 1999; Lizuka et al., 2000; Murtugudde et al., 2000; Yamagata et al., 2002).

Several studies (Mutai et al., 1998; Clark, 2003; Behera et al., 2005) have found the short rains of eastern Africa to be strongly related to the IOD. Research by Jury et al. (2002) on the IOD shows that the east African rainfall regime shares maritime convection with the IO, while convection over southern Africa is inversely related. Our preliminary results indicate that most of the positive IOD events from 1958 (the IOD data period available) are associated with subnormal seasonal rainfall over Zimbabwe.

1.4 Darwin Sea Level Pressure (SLP)

The overwhelming influence of the IOD is not only in the western IO but also in the eastern IO, where its main domain of influence includes Darwin SLP (Behera and Yamagata, 2003; Behera et al., 2005). Darwin also forms part of the western pole of the SO, which is the atmospheric component of ENSO. In view of this, Darwin SLP then becomes an interesting element to study, not just because of the impressive continuous and homogeneous pressure anomaly data for the 100 year study period, but also because it has a strong signature in both the ENSO and IOD events. The assumption is that if both phenomena influence droughts over the sub-region, then Darwin SLP should possess predictive properties common to both ENSO and IOD. An attempt is made to establish Darwin SLP's superior association with Zimbabwe droughts, from a prediction point of view. Therefore, ways in which Darwin SLP anomalies influence Zimbabwe seasonal rainfall in conjunction with (and independent of) ENSO during the 20th century are explored. The stability of these relationships during this period, especially how the tropical climate shift of 1976 could have influenced this century long association, is investigated. Figure 1 shows the location of areas referred to in this study.

2. Data and analysis

2.1 Rainfall data

A 100 year time series of aerially averaged seasonal rainfall (1901–2000) for Zimbabwe was obtained from the Zimbabwe Meteorological Services Office. The seasonal rainfall data are for the months October to March. These were derived from the average of ten rainfall stations with rainfall time series exceeding 100 years and located across the country. The country area-averaged rainfall data were considered to improve the signal to noise ratio, compared to the use of individual station data.

2.2 ENSO data

The Southern Oscillation Index (SOI), as well as standardised monthly SLP datasets for Darwin, were provided by the NOAA, National Weather Service, Climate Prediction Center website. The standard ENSO phases for the century long study period are derived from the Japan Meteorological Agency (JMA) http://www.coaps.fsu.edu/products/jma_index.php.

2.3 The IO Sea Surface Temperatures (SSTs)

The IO and Pacific SST processed files were downloaded from the NOAA ftp site and cover the period 1950 to 2001. The spatial sea surface temperature data were extracted from the area that covers the tropical Indian and Pacific Oceans (Fig. 5a and b).

2.4 The Standardised Precipitation Index method (SPI)

The SPI method is used as it is able to return fundamental parameters in the analysis of occurrence of different drought types over the last century in terms of severity, magnitude and frequency. These are the parameters that are of major concern in drought prediction. McKee et al. (1993) developed the Standardized Precipitation Index (SPI) for the purpose of defining and monitoring drought, and this has become the most widely used drought index (Vicente-Serrano, 2005). Conceptually, the SPI is equivalent to the Z_{score}, which is often used in statistics. A comprehensive method for computing the index can be found in Guttman (1999).

The SPI calculation is similar to a Z_{score} which is calculated as $Z_{\text{score}} = \frac{R-\overline{R}}{\sigma}$, where Z_{score} expresses the seasonal rainfall (R) score distance from the seasonal average $\overline{R}$ in standard deviation (σ) units. Since typical rainfall data are positively skewed, a pre-adjustment to this standard Z_{score} formulation becomes necessary. This is done by transforming the rainfall data to a more normal or Gaussian symmetrical distribution by applying the gamma function. After the rainfall data have been transformed, the SPI is calculated in a manner that mirrors the Z_{score} and may be interpreted similarly. Thus, the value of the SPI becomes the number of standard deviations above or below the seasonal mean. Theoretically, the SPI is unbounded empirically but it is extremely rare to observe values greater than +0.3 and less than −0.3. In this study, the rainfall time series is for the time scale of six months (October to March), which constitute the rainfall season for Zimbabwe. The Zimbabwe seasonal SPI values (Zim SPI) are calculated using an SPI program available at http://www.drought.unl.edu/monitor/SPI/program/program. The SPI is positive for a seasonal rainfall surplus over the 100 year mean and negative for a deficit. The degree of negative deviation is an indicator of drought and the reverse is true for a positive deviation.

The values of the Zim SPI, their frequency probabilities and nominal class descriptions are provided in Table 1. The Zim SPI nominal classification is done using the Agnew (1999) SPI scale that uses the 5%, 10% and 20% occurrence probability. However, this Agnew scale is modified as it classifies some historical regional rainfall seasons as normal but were in fact documented as droughts/wet seasons. Thus, in adapting the scale to the region the 33.3% (tercile) occurrence probability is included, which is traditionally used within the southern African region to define drought/wet season thresholds. In this way another class of mild drought/slight wet seasons is added to the original Agnew scale. The new scale

Table 1. Seasonal rainfall classification by Zim SPI value and corresponding event probabilities according to Agnew (1999). Note that the 21–33.3% occurrence probabilities (in italics) have been added to the Agnew classification so as to accommodate the tercile (33.3%) method used to classify wet and dry seasons over the southern African region

SPI value occurrence	Occurrence (%)	Nominal SPI class
>1.645	≤5	Extremely wet
1.644 to 1.282	6–10	Severely wet
0.842 to 1.281	11–20	Moderately wet
0.524 to 0.841	*21–33*	*Slightly wet*
−0.523 to 0.523	34–50	Normal
−0.841 to −0.524	*21–33*	*Mild drought*
−1.281 to −0.842	11–20	Moderate drought
−1.644 to −1.282	6–10	Severe drought
< −1.645	≤5	Extreme drought

shown in Table 1. Note that Table 1 also shows that the Zim SPI is symmetrical for the occurrence of wet and dry seasons.

2.5 Darwin pressure anomaly index calculation

Four-month averages are used in order to remove non-representative transient and local effects and obtain at least seasonal values for the index for SOI and Darwin pressure anomalies. The correlation functions between Zim SPI and each of the two indicators, the SOI and Darwin sea level pressure anomalies, are calculated by starting with the indicator's four-month averaged time series from January to April (JFMA) and then sliding it up by one month to the averaged September to December (SOND) period. The averaged period has been chosen to include the first part of the regional rainfall season, October to December (OND). This is expected to provide the monthly time evolution of the relationships of the two indicators of interest prior to and including at least the first part of the rainfall season.

The highest significant association, which offers the longest lead-time, of the four-month averaged Darwin pressure anomalies is further converted into an index and categorised. High positive (negative) values $\geq +0.6$ (≤ -0.6), represent the high positive (negative) Darwin phase of the index and the values in between represent the neutral phase. The methodology is analogous to the determination of El Niño, La Niña and Neutral phases of the ENSO index. Thus, we have High Positive and Negative Phases representing the averaged Darwin pressure anomaly extreme phases of the cycle just as El Niño and La Niña represent the extreme phases of the ENSO cycle.

3. Results and discussion

3.1 Comparing lead times of Darwin pressure anomalies and ENSO

Correlation analysis is used to identify the period lags for which the SOI and Darwin pressure anomalies are significantly correlated with Zim SPI. It is also a strategy to determine the longest lead-time to the onset of Zimbabwe summer rainfall season. Progressively lagged four-month averaged Darwin pressure anomalies and the SOI are correlated with Zim SPI with the results shown in Fig. 2.

The correlation patterns show the consistently negative and positive association of Zim SPI with the Darwin pressure anomalies and the SOI, respectively. The Tahiti pressure anomaly correlation with Zim SPI has not been included in the diagram as the association is similar to that of the SOI but less pronounced. The association of Zim SPI and Darwin is statistically significant throughout the period of concern except for JFMA but the SOI-Zim SPI relationship becomes significant (above the 99% confidence level) from the averaged AMJJ period. The Zim SPI correlation with Darwin and the SOI brings out not only the variability but also the significantly different temporal evolution of SLP in the eastern IO and

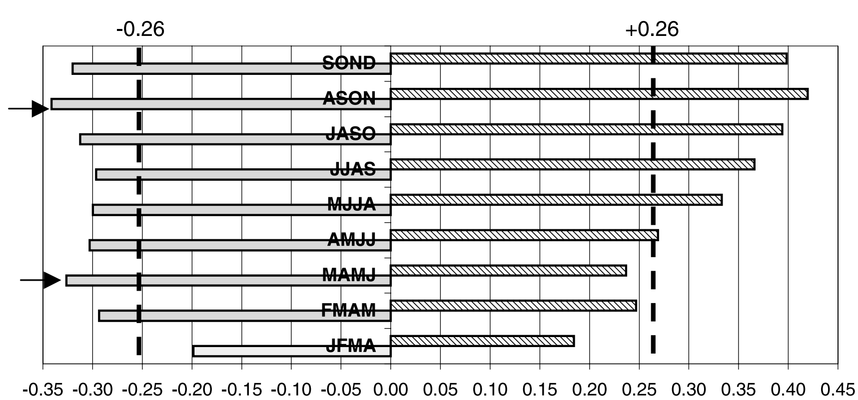

	JFMA	FMAM	MAMJ	AMJJ	MJJA	JJAS	JASO	ASON	SOND
SOI	0.184	0.247	0.237	0.269	0.333	0.366	0.394	0.420	0.398
Darwin	-0.198	-0.293	-0.326	-0.303	-0.300	-0.297	-0.312	-0.341	-0.320

Fig. 2. Correlations between Zim SPI and four-month averaged values of pressure anomalies at Darwin as well as SOI (ENSO index). (Threshold value of correlation coefficient is ± 0.26 at the 99% confidence level for the 100-year time series)

the equatorial Pacific. However, the earlier relationship suggests the existence of IO SLP oscillations that exhibit significant dual maximal correlations (Fig. 2). No direct physical relationship between the Zim SPI and Darwin pressure anomalies at such relatively long lags, especially with the first peak, is plausible.

Figure 2 also shows that Darwin has its initial peak correlation of −0.33 (significant above the 99% confidence level) for MAMJ, four months prior to October, the month for the earliest onset of the Zimbabwe rainfall season. An equally strong correlation for Zim SPI and SOI is realised two months later for the period MJJA. (Note that the MJJA is the averaged period normally used at SARCOF for sub regional seasonal forecasts which are issued in mid-September.) However, both SOI and Darwin anomalies have maximum associations with Zim SPI simultaneously for the averaged period August to November (ASON). Both correlations tend to be strongest at the beginning of the rainfall season but gradually weaken as the SLP anomalies coincide with the main rains of the season (DJFM).

It is then determined that the most useful antecedent parameter with the longest lead-time between the two time series investigated appears to be the trend of Darwin SLP anomaly for the averaged period of MAMJ. Although it is quite evident that the Zim SPI-Darwin relationship is significantly different from the Zim SPI-SOI association, it has to be recognised that Darwin directly influences ENSO as it forms the other pole of the SOI.

3.2 Relationship between the Zim SPI and the MAMJ Darwin index

The nature of the statistical linear relationship between Zim SPI and Darwin has been established using the correlation method. However, this method only captures the phase relationship thus prompting further investigation to confirm the corresponding amplitude variation. Thus, in this section we analyse the amplitude association between Zim SPI and MAMJ Darwin SLP anomalies, particularly during the extreme years. A graph drawn for the closer investigation of the relationship of the two time series is shown in Fig. 3. The Zim SPI with the positive values represent the relative magnitude of excess seasonal rainfall, and the negative shows the relative seasonal deficit. The corresponding pressure anomalies of MAMJ Darwin are also shown.

The inter-annual variations of MAMJ Darwin and Zim SPI series show some seemingly random fluctuations. When both are smoothed using a five-year filter the variability reveals inversely related alternate epochs of above and below normal regimes. This suggests that the occurrence of a positive MAMJ Darwin phase tends to enhance the Zimbabwe seasonal rainfall and the negative phase diminishes it. The most notable feature of these two indices is the year-to-year persistence that characterises much of their variability in the 20th century. This long-lived persistence is also highlighted by the 5-year running averages of the indices. Of note during the century is the longest period from the late 1970s when the Zim SPI is

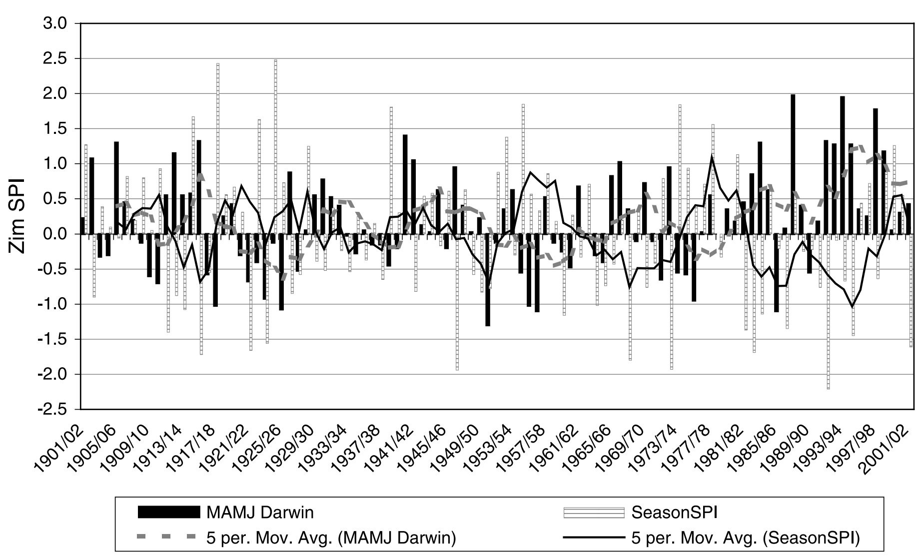

Fig. 3. The variation of the Zim SPI and MAMJ Darwin SLP anomaly time series. Corresponding series have been smoothed using a five-year filter

predominantly negative while the MAMJ Darwin is predominantly positive.

It can be noted from Fig. 3 that this inverse relationship is more pronounced in extreme MAMJ Darwin and the corresponding Zim SPI relationship. About 10 of the 15 (67%) high negative MAMJ Darwin phases coincide with seasonal rainfall excesses (positive Zim SPIs), but more interesting is the coincidence of 24 of 29 (83%) of high positive MAMJ Darwin phase (see also Table 2) with seasonal rainfall deficits.

3.3 The superior role of MAMJ Darwin over El Niño as a major simple drought predictor

We shall refer to high positive MAMJ Darwin SLP anomalies simply as MAMJ Darwin. The hit rate of 83% of MAMJ Darwin with Zimbabwe seasonal rainfall deficits is by any standard very high. Therefore, we further compare this performance with that of ENSO which is the traditional simple drought prediction index used over the sub-region. It should be noted that these two are independent events but they do co-occur at various times. This prompts the separation of the co-occurring events so as to assess each event in its individual capacity (i.e. without the influence of the other). This is also done in order to avoid the expected mis-interpretation that the Darwin SLP anomalies are just the result of ENSO. In this endeavour, we extract 'pure' MAMJ Darwin events which occur during non-ENSO years, 'pure' El Niño events, which occur without the pre-occurrence of MAMJ Darwin and then the co-occurrence events, when high MAMJ Darwin occur during El Niño years. Hence the performance of these three events is then measured against individual coincidences with the season's nominal classification of Zim SPI (Table 1) (according to its influence an dryness or wetness).

It is interesting to note that when these two events, MAMJ Darwin and El Niño, are analysed concurrently, the hit rate significantly improves with increased sub normal seasonal rainfall. For example, they coincide with ≥60% of seasonal rainfall deficits, (28 out of 47), 65% of slight drought or worse (20 out of 31), 75% of moderate droughts or worse, 70% of severe droughts or worse, and finally 71% of extreme droughts of the century (5 out 7). The remaining percentages are accounted for by other events. This shows that these events are more strongly linked to atmospheric processes, which considerably suppress seasonal rainfall activities, than to all other events.

Figure 4 shows how these events, in their pure form as well as in co-occurrences, coincide with the Zim SPI. The solid lines above and below the x-axis demarcate the moderately wet and drought categories, respectively. It is interesting to observe that 'pure' El Niño events coincide more with rainfall surpluses than droughts, but when accompanied by MAMJ Darwin, the coincidences with droughts become predominant. Likewise 'pure' MAMJ Darwin events coincide with more

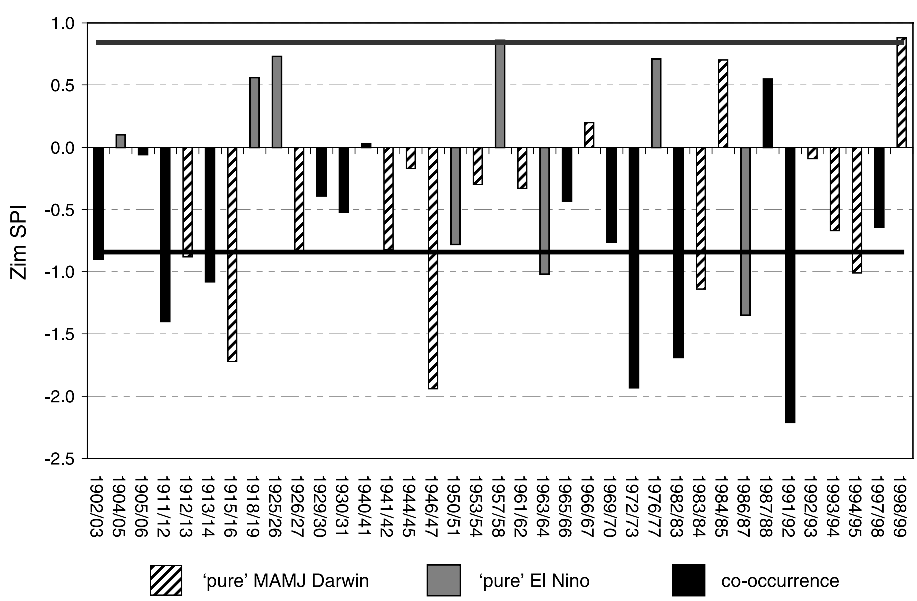

Fig. 4. Zim SPI relative to pure' El Niño 'pure' MAMJ Darwin and co-occurrence events. The graph includes all the events that occurred during the period 1901–2000. Negative values of Zim SPI indicate seasonal rainfall deficits and positive values represents excesses. The solid lines indicate the moderate drought and wet season Zim SPI thresholds

Table 2. Cross tabulation of the event composites with their respective Zim SPI nominal class. (Note that other events have been added to account for other unspecified events)

	Darwin high phase	El Niño phase	'Pure' Darwin	'Pure' El Niño	Co-occurrences	Other events	Century total
Extreme drought	5	3	2	0	3	2	7
Severe drought	1	2	0	1	1	1	3
Moderate drought	6	3	4	1	2	2	9
Slight drought	4	3	2	1	3	6	12
Normal dry	8	4	4	0	4	8	16
Normal wet	2	2	1	1	0	15	17
Slightly wet	2	4	1	3	1	12	17
Moderately wet	1	1	1	1	0	8	10
Severely wet	0	0	0	0	0	3	3
Extremely wet	0	0	0	0	0	6	6
Total deficits	24	15	12	3	13	19	47
Century total events	29	22	15	8	14	63	100
Seasonal deficits/total events (%)	83%	68%	80%	38%	93%	30%	47%

droughts. The most important observation here is that during the occurrence of these events, whether in isolation or otherwise, it is extremely rare for corresponding Zim SPI values to exceed the slightly wet threshold. Only two barely exceed the moderately wet threshold (see Fig. 4).

A more detailed analysis is presented with the aid of Table 2. Here, the performance of the three events is clearly illustrated as well as the superiority of MAMJ Darwin over El Niño. MAMJ Darwin, in general, has 83% coincidences with seasonal rainfall deficits of the century. Similar calculation with El Niño shows that only 68% of the El Niño years coincide with seasonal rainfall deficits. It is interesting to note that co-occurrences of the two events have overwhelming coincidences with seasonal rainfall deficits, with 13 out of 14 (93%) events. Nevertheless, the suppression of the seasonal rainfall total for the remaining co-occurrence event is evident as it is classed only within the slightly wet category. On the other hand, the independent El Niño has a low coincidence rate of 3 out of 8 (38%) with seasonal rainfall deficits.

As far as linking the seven extreme droughts of the century is concerned, these 'pure' El Niño events seem not to be ralated. They do not coincide with any (0%) extreme droughts during the century. Two droughts coincide with 'pure' Darwin, three with co-occurrences and the remaining two with yet unspecified events. Once again, co-occurrences are dominant with 'pure' El Niño being the least influential. Table 2 shows these events along with their corresponding Zim SPI nominal classification.

In order to assess the average seasonal performance during the three events, event composites are constructed for 'pure' El Niño, 'pure' Darwin and co-occurrences. Table 3 shows the mean values of the Zim SPI during the respective event composites as well as their nominal classification. It can be seen that the co-occurrence event composite has the moderate drought, followed by 'pure' Darwin with slight drought. On average the 'pure' El Niño event composite has a small negative value (close to zero), which is classified as normal dry.

Table 3. Composites for 'pure' MAMJ Darwin, 'pure' El Niño and co-occurrence events during the 20th century showing the mean Zim SPI classification

Event composite	Number of seasons in the composite	Mean Zim SPI	Mean Zim SPI classification
'Pure' MAMJ Darwin	15	−0.54	Slight drought
'Pure' El Niño	8	−0.02	Normal dry
Co-occurrence	14	−0.84	Moderate drought

We also investigated the sensitivity of this approach to the precise index of ENSO used to define the phases. We checked with the Niño 3.4, Niño 3, as well as the multi-variate ENSO index (http://www.cdc.noaa.gov/people/klaus.wolter/MEI/) and concluded that the results are largely insensitive to the precise ENSO index. Analysis of the opposite phase relationships with ENSO and MAMJ Darwin are beyond the scope of this study as we are only interested in seasonal rainfall deficits.

3.4 Linking MAMJ Darwin SLP anomalies and Zim SPI to the tropical IO SSTs

In this section we analyse the correlation coefficient patterns for Zim SPI and MAMJ Darwin SLP anomalies with respect to SOND SST data for the tropical Indian and Pacific regions. We specifically selected for analysis the averaged period of SOND so as to coincide with the period when the IOD and ENSO are at their peak (e.g. Yamagata et al., 2003). Consequently, the link, which has been missing between MAMJ, Zim SPI and the tropical IO SSTs, becomes apparent.

Figure 5a and b show a simple correlation structure of Zim SPI with SSTs in the Indian and Pacific regions that resembles closely the IOD and ENSO in their respective basins. Another way of interpreting the results is that the rainfall anomalies of southern Africa are related significantly to the two phenomena. In other words, rainfall deficits are associated with the warming of the west IO and east Pacific as well as cooling of the east IO. One can conclude that IOD events occur as part of ENSO as postulated by Banquero-Bernal et al. (2002). As a result, one concern immediately emerges; whether IOD is independent from ENSO in its influence. This debate is beyond the scope of this work. Of importance here is that, MAMJ Darwin and Zim SPI map significant correlation coefficients of IOD and ENSO-like patterns with the SOND averaged SSTs in the IO and Pacific, respectively. Hence, MAMJ Darwin can predict to some extent, the IOD as well as ENSO.

We also note that the correlation coefficient values are higher over the IOD than over the ENSO SST region in the Pacific. Both MAMJ Darwin and Zim SPI have higher significant correlation coefficient (above 95% significant level) values that are by far more extensive over the western region of the IO than over the eastern region. However, the magnitude of the correlation coefficients in the IO is generally higher for the MAMJ Darwin SLP anomalies than for Zim SPI. Therefore, it may now become highly probable that the MAMJ Darwin SLP anomalies are linked to the Zimbabwe seasonal rainfall variability through processes taking place in the tropical IO, especially the western region.

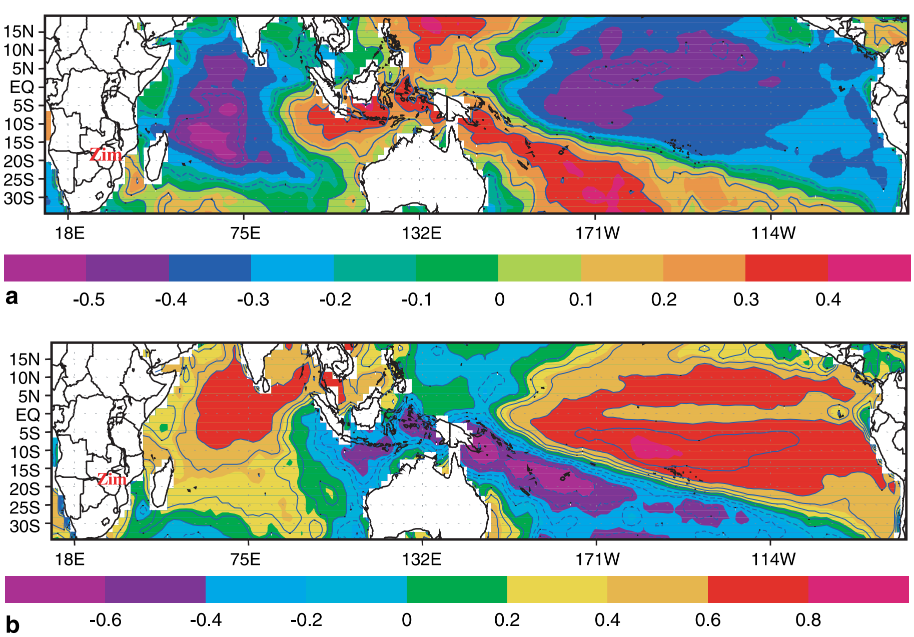

Fig. 5. Correlation coefficient patterns for Zim SPI (**a**) and MAMJ Darwin SLP anomalies (**b**) with SOND SST data for the region of the Pacific and IO (1951 to 2000). Threshold correlation coefficient values of ± 0.37 and ± 0.27 are statistically significant at the 99% and 95% confidence levels, respectively, using a two-tailed *t*-test. Note that the dipole SST pattern in the IO is clearly visible

3.5 Temporal stability of the Darwin anomalies and ENSO during the 20th century

In this section we investigate the temporal stability of Darwin pressure anomalies and ENSO during the century. This is crucial should developing a better predictive scheme become necessary. Since any predictive scheme depends on the stability of the empirical relationship of the predictor and the predictand over time, we evaluate the temporal stability of the association of Zim SPI with the SOI and MAMJ Darwin. We notice that the most probable factor which could have affected these relationships significantly over the century is the well-documented 1976 climate shift (Trenberth, 1990; Graham, 1994; Terray, 1994; Wang, 1995; Trenberth and Hoar, 1996; Behera et al., 2005) in which there were significant SST increases found in the tropical oceans including the IO. Therefore, we initially look at how this shift affected the SOI and Darwin SLP in their individual capacity before investigating the effects on their relationships with Zim SPI.

Figure 6a shows the time series of MJJA and SOI and illustrates that the climate shift has simultaneously affected the structure and evolution of ENSO whereby more El Niño and fewer La Niña events occured than in the pre-climate shift period (see more negative SOI anomalies in Fig. 6b), (Trenberth, 1990; Trenberth and Hoar, 1996; Clark et al., 2000; Behera et al., 2005). Darwin responded by having higher positive pressure anomalies of unprecedented levels for the century (which are clearly visible in Fig. 6a) with only two events of negative pressure anomalies after the shift.

The strength of MAMJ Darwin SLP anomalies decreased until the mid 1970s when a sudden rise ensued. This may be in conjunction with a shift to a cooler state in the tropical western Pacific after the 1976 climate shift. This discontinuity in the trend is confirmed by the least squares linear trend imposed on the period prior to and after the climate shift. The first period shows a negative trend while the latter illustrates a jump to a noticeably higher mean as well as a conspicuous reversal in trend to positive. The effects of this climate shift seem not to be that apparent for the MJJA SOI time series (Fig. 6b). However,

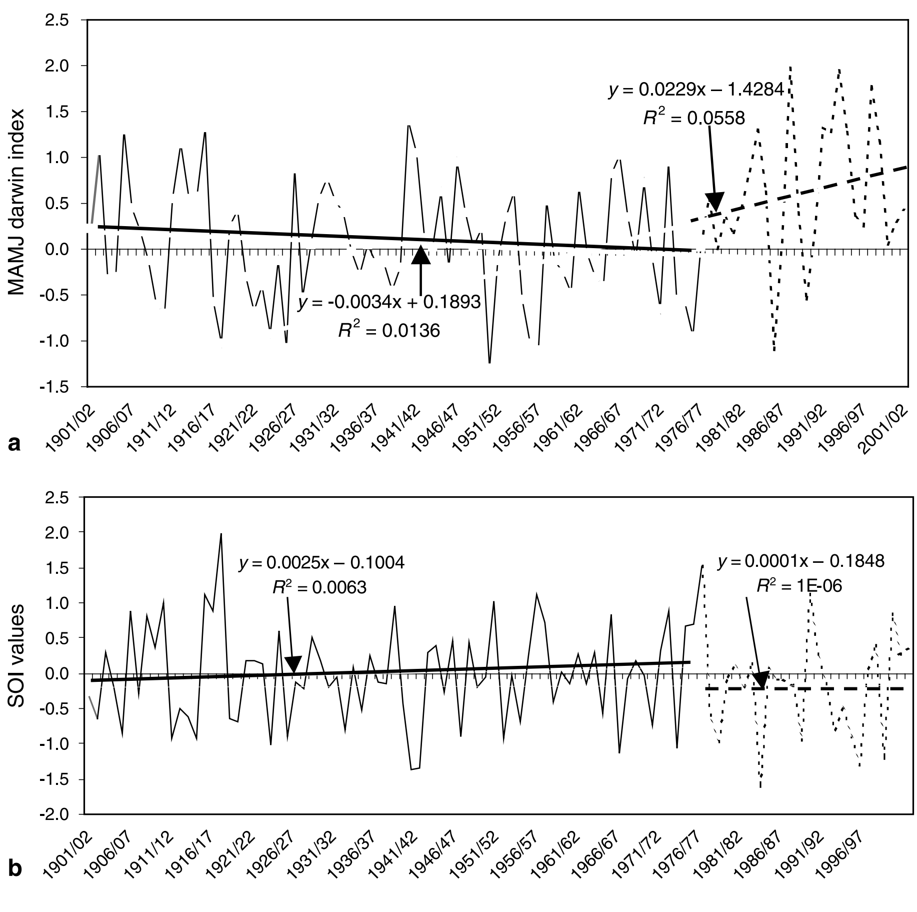

Fig. 6. Time series of MAMJ Darwin SLP anomalies (**a**) and the MJJA SOI (**b**) for the period 1901–2002. The solid line is the linear least squares fit for the time series from 1901 to 1975 and the right side dashed line is for 1976 to 2002

the SOI values seem to have been lower after the climate shift than during the earlier part of the record with the post-shift mean clearly below the century average (Fig. 6b).

3.6 Stability of the statistical association of Zim SPI with ENSO and MAMJ Darwin

We have shown that the climate shift has affected the trends of MAMJ Darwin as well as the SOI differently. Therefore we need to investigate how this has influenced the statistical association of Zim SPI with the SOI and MAMJ Darwin SLP anomalies separately. We use a five-decade sliding window of the respective correlation coefficients to investigate the stability of these relationships during the century.

The magnitude of both correlations, Zim SPI-ENSO and Zim SPI-MAMJ Darwin, over the century coincides at 0.3. However, the 51-year sliding correlation coefficient values for the two pairs of association are not stable as they exhibit relatively wide temporal variations during the century (Fig. 7). The time evolution of these relationships brings out well, among others, the noticeable effect of the 1976 climate shift. The moving correlation values show the significant relationship (above 95% significant level) between SOI and Zim SPI that has been observed for the greater part of the 20th century, appear to have been diminishing, especially in the recent three decades (see negative trend line for SOI). At the same time the association with MAMJ Darwin SLP anomalies has suddenly become predominantly significant during the last three decades (Fig. 7). This is most probably due to the effect of the observed climate shift.

The Zim SPI-MAMJ Darwin relationship has, for the first time during the century, closely matched the Zim SPI-SOI relationship following the climatic shift and has essentially maintained that trend up to the end of the century (Fig. 7). Note that the dominant correlation of Zim SPI with JJAS SOI over that of Zim SPI with MAMJ Darwin pressure anomalies does not show ENSO superiority in influencing droughts. The Zim SPI-MJJA SOI higher correlations only captures phase relationships that are relatively stronger for both positive and negative phases. Zim SPI-MAMJ Darwin correlations appear to be weaker because, as mentioned earlier, the Zim SPI is particularly sensitive to only one phase of the MAMJ Darwin pressure anomalies. It is only the rarely occurring positive extremes of MAMJ Darwin pressure anomalies that are closely related to seasonal rainfall deficits but the negative extremes do not show any particular influence on seasonal rainfall excesses. This is the reason, which has prompted further investigation, for checking the corresponding amplitude variations, despite having performed the correlation analysis.

However, the climate shift seems to have improved the phase relationships by strengthening the general Zim SPI association with MAMJ Darwin pressure anomalies. At the same time, the climate shift appears not to have significantly altered the association of the Zim SPI with the SOI. While these relationships are susceptible to

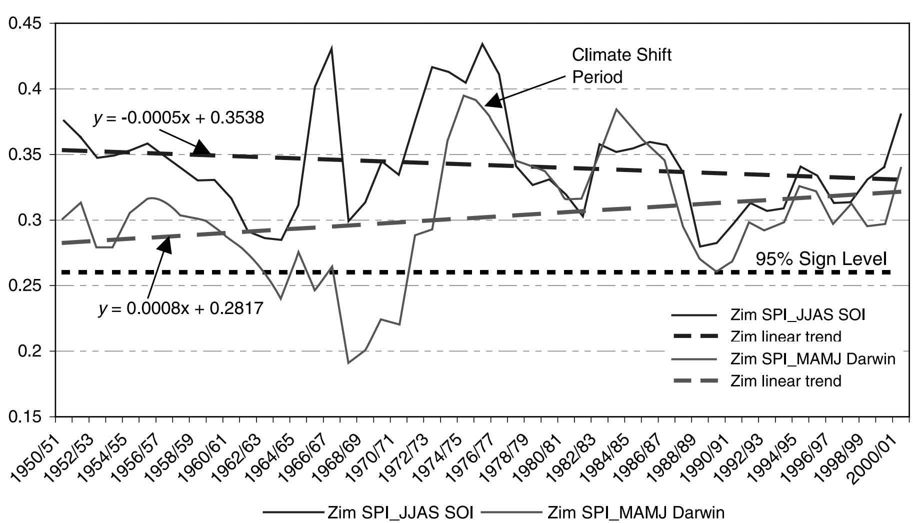

Fig. 7. 51-year sliding correlation coefficients between Zim SPI and ENSO index (SOI, solid line) and those between Zim SPI and MAMJ Darwin (dashed; to be multiplied by −1) during the period 1901–2000. Least squares linear trend lines have been added to show the century trend of the correlations. The significant correlation value at 95% significant level is 0.27 for a 2 tailed student's distribution

decadal changes, the least squares linear trend on the two series show a noticeable rising trend for the Zim SPI-MAMJ Darwin relationship and a falling trend for the Zim SPI-SOI trend (Fig. 7).

The climate shift is seen here to have altered significantly the relative correlation structures between Zim SPI and MAMJ Darwin but is not that obvious for the Zim SPI and ENSO. This is consistent with our observation that the climate shift is mainly reflected by pressure rise at Darwin rather than the SOI itself. Todd and Wallace (2003) also reached similar conclusions by noticing that the resulting lower values of the SOI in the past few decades were the result of pressure at Tahiti that has not fallen as noticeably as the rise in Darwin SLP pressure.

4. Conclusions and recommendations

The MAMJ Darwin is an earlier and more skillful predictor of Zimbabwean droughts than the JJAS SOI, which is traditionally used during Southern African Regional Climate Outlook Forums (SARCOFs) for the SADC countries. Thus, this finding has clear implications for the importance of Darwin pressure anomalies in southern African seasonal drought forecasting efforts. It is quite apparent from this work that the previously assumed authority of El Niño in influencing droughts of eastern southern Africa failed to show up in this regard. We seem to have successfully challenged this widely accepted view by proposing the influence of MAMJ Darwin SLP anomalies instead.

The changes in MAMJ Darwin SLP anomalies have proved to be more important in their association with Zimbabwe droughts than the variability of ENSO itself. In the absence of ENSO, the MAMJ Darwin SLP anomalies can still provide much of the skill in drought forecasts for southern Africa. However, this skill collapses with the exclusion of MAMJ Darwin years. Therefore, it is possible that the atmospheric circulation anomalies induced by the impact of MAMJ Darwin SLP anomalies is connected to prime atmospheric processes that exert a much more marked influence on southern African droughts than the idealised remote ENSO forcing from the Pacific.

The proposition of yet another climate mode is supported by the mere demonstration that both the MAMJ Darwin SLP anomalies and Zim SPI are significantly correlated to the IOD. With this knowledge, it is now arguable that the more severe droughts being experienced over southern Africa in recent years can still be attributed to ENSO in the global perspective and not essentially to the events of the adjacent tropical IO SSTs. This is further supported by the observed significant modifications of the association between Zim SPI and MAMJ Darwin SLP anomalies due to the climate shift of 1976, which largely changed the IO SST background. It has apparently made the Zim SPI-MAMJ Darwin relationship more significant in recent decades but has not significantly changed the Zim SPI-ENSO relationship.

El Niño alone, without prior occurrence of MAMJ Darwin, has proved to be ineffective in influencing the more severe droughts during the century. On the other hand, the influence on subnormal rainfall is significantly enhanced during co-occurrences. Thus, MAMJ Darwin influences Zimbabwe seasonal rainfall on its own and apparently strengthens the influence of the El Niño on droughts in co-occurrences. Therefore, in previous work, the role of El Niño in influencing southern African droughts was largely amplified by the numerous co-occurrences with the MAMJ Darwin events. It would appear that with this knowledge what matters most in the prediction of the droughts over central southern Africa is no longer the traditional El Niño signal, but the evolution of MAMJ Darwin events. Thus, the predictability of severe droughts solely based on the El Niño state with no prior knowledge of the Darwin pressure anomalies would not yield any better skill.

In view of the increasing correlation between Zim SPI and MAMJ Darwin SLP anomalies, it may be worth examining the possibility of using it for the climate prediction process of southern African rainfall deficits. With a longer lead-time than ENSO, MAMJ Darwin can be used as a potential simple predictor to determine the probability of the occurrence of droughts four months on or to the onset of the rainfall season. The consistent and skillful simple prediction of droughts for the century long data cannot be a product of chance. This may provide an opportunity to predict seasonally averaged drought conditions for southern African at longer lead-times. While a skillful forecast of this type is of marginal use to the individual farmer, it would be of significant value to national planners and decision-makers. It is important to note that, combining ENSO and MAMJ Darwin SLP anomalies offers improved statistical drought predictions over those based solely upon one of these two climate events.

However, it is necessary to substantiate the current findings as well as to understand the physics behind the evolution of MAMJ Darwin pressure anomalies and how other processes enhance or supress it, using Global Circulation Models. These may provide the link with IOD as well. Other droughts that are neither related to the MAMJ Darwin SLP anomalies nor to ENSO also need to be investigated in a bid to assess their predictability. All in all, these results reinforce the importance of investigating the physical existence/non-existence of non-ENSO processes that are directly linked to drought occurrence in southern Africa.

Acknowledgement

The authors wish to thank the Zimbabwe Meteorological Department for providing the rainfall data. The preparation including writing of this manuscript benefited from the support (including financial) rendered by University Network for Disaster Risk Reduction in Africa (UNEDRA), ITC United Nations University (UNU) and the University of Johannesburg. The institutions actively support disaster related research in African Universities. Professor Harold Hannegarn and Tsehaie Woldai are thanked for their useful advise. The anonymous reviewer is greatly thanked for the valuable comments and insights to this paper. Bindura University is also thanked for partially financing and providing facilities at the University.

References

Agnew CT (1999) Using the SPI to identify drought. Drought Network News 12(1): 6–12

Allan R, Chambers D, Drosdowsky W, Hendon H, Latif M, Nicholls N, Smith I, Stone R, Tourre Y (2001) Is there an Indian Ocean Dipole, and is it independent of the El Niño – Southern Oscillation? CLIVAR Exchanges 6: 18–22

Ashok K, Guan Z, Yamagata T (2003) Influence of the Indian Ocean Dipole on the Australian Winter rainfall. Geophys Res Lett 30: 1821 (doi: 10.1029/2003GL017926)

Baquero-Bernal A, Latif M (2002) On dipole-like variability in the tropical Indian Ocean. J Climate 15(11): 1358–1368

Behera SK, Yamagata T (2003) Influence of the Indian Ocean dipole on the Southern Oscillation. J Meteor Soc Japan 81(1): 169–177

Behera SK, Luo J, Masson S (2005) Paramount impact of the Indian Ocean Dipole on the East African Short Rains. J Climate 18(21): 4514–4530

Cane MA, Eshel G, Buckland RW (1994) Forecasting Zimbabwean maize yields using eastern equatorial Pacific sea surface temperature. Nature 370: 204–205

Chambers DP, Tapley BD, Stewart RH (1999) Anomalous warming in the Indian Ocean coincident with El Niño. J Geophys Res 104: 10523–10533

Clark CO, Cole JE, Webster PJ (2000) Indian Ocean SST and Indian summer rainfall: predictive relationships and their decadal variability. J Climate 13: 2503–2519

Clark CO, Webster PJ, Cole JE (2003) Interdecadal variability of the relationship between the Indian Ocean zonal mode and East African coastal rainfall anomalies. J Climate 16: 548–554

Fauchereau N, Trazaska S, Rouault M, Richard Y (2003) Rainfall variability and changes in southern Africa during the last 20^{th} century in the Global Warming context. Nat Hazards 29: 139–154

Graham NE (1994) Decadal-scale climate variability in the 1970s and 1980s: observations of model results. Clim Dynam 10: 135–159

Guttman NB (1999) Accepting the Standardized Precipitation Index: a calculation algorithm. J Amer Water Resources assn 35: 311–322

Iizuka S, Matsuura T, Yamagata T (2000) The Indian Ocean SST Diploe simulated in coupled general circulation model. Geophys Res Lett 27: 3369–3372

Jury MR, Enfield DB, Me'lice J (2002) Tropical monsoons around Africa: stability of El Niño Southern Oscillation associations and links with continental climate. J Geophys Res 107(C10): 3151 (doi: 10.1029/2000JC000507)

Jury MR, Mwafulirwa ND (2002) Climate variability in Malawi. Part 1: Dry summers, statistical associations and predictability. Int J Climatol 22(11): 1289–1302

Landman WA, Mason SJ (1999) Change in the association between Indian Ocean sea-surface temperatures and summer rainfall over South Africa and Namibia. Int J Climatol 19(13): 1477–1492

Makarau A (1995) Intra-seasonal oscillatory modes of southern African African summer circulation. PhD thesis, University of Cape Town

Mason SJ (1997) Recent changes in El Niño-Southern Oscillation events and their implications for southern African climate. Transact Roy Soc South Africa 52: 377–403

Matarira CH (1990) Drought over Zimbabwe in a regional and global context. Int J Climatol 10: 609–625

McKee TB, Doesken NJ, Kleist J (1993) The relationship of drought frequency and duration to time scale. In: Eighth Conference on Applied Climatology, Anaheim, CA (USA), pp 179–184

Murtugudde R, McCreary JP Jr, Busalacchi AJ (2000) Oceanic processes associated with anomalous events in the Indian Ocean with relevance to 1997–1998. J Geophys Res 105: 3295–3306

Mutai CC, Ward MN, Colman AW (1998) Towards the prediction to the East Africa Short rains based on sea surface temperature-atmosphere coupling. Int J Climatol 18: 975–997

Nicholson SE, Leposo L, Grist J (2000) The relationship between El Niño and drought over Botswana. J Climate 14: 323–335

Ogallo L, Janowiak E, Halpert MS (1988) Teleconnections between seasonal rainfall over east Africa and global seas surface temperature anomalies. J Meteor Soc Japan 66: 807–821

Paulo AA, Ferreira E, Pereira LS (2005) Stochastic prediction of SPI drought class transitions ICID 21st European Regional Conference – May 2005 – Germany and Poland

Phillips J, Cane MA, Rosenzweig C (1998) ENSO, seasonal rainfall patterns and maize yield variability in Zimbabwe. Agric Forest Meteor 90: 39–50

Rasmusson M, Eugene EM (1987) Global climate change and variability: effects on drought and desertification in Africa, WMO, Papers presented at the regional Seminar Addis Ababa November 1985, pp 1–32

Reason CJC (1999) Interannual warm and cool events in the subtropical: mid-latitude South Indian Ocean region. Geophys Res Lett 26: 215–218

Reason CJC, Mulenga H (1999) Relationships between South African rainfall and SST anomalies in the south West Indian Ocean. Int J Climatol 19: 1651–1673

Reason CJC, Allan RJ, Lindesay JA, Ansell TJ (2000) ENSO and climatic signals in the Indian Ocean basin in the global contex. Part 1: Inter-annual composite patterns. Int J Climatol 20: 1285–1327

Richard Y, Fauchereau N, Poccard I, Rouault M, Trzaska S (2001) 20th century droughts in southern Africa: spatial and temporal variability, teleconnections with oceanic and atmospheric conditions. Int J Climatol 21: 873–885

Rocha A, Simmonds I (1996) Interannual variability of South-eastern African summer rainfall. Part I: Relationships with air-sea interaction processes. Int J Climatol 17(3): 235–265

Ropelewski CF, Halpert MS (1987) Global and regional-scale precipitation patterns associated with the El-Niño/Southern Oscillation. Mon Wea Rev 115: 1606–1626

Rouault M, Richard Y (2005) Intensity and spatial extent of droughts in southern Africa. Geophys Res Lett 32: L15702 (doi: 10.1029/2005GL022436)

Saji NH, Goswami BN, Vinayachandran PN, Yamagata T (1999) A dipole mode in the tropical Indian Ocean. Nature 401: 360–363

Shinoda M, Kawamura R (1996) Relationships between rainfall over semi-arid southern Africa and geopotential heights, and sea surface temperatures. J Meteor Soc Japan 74: 21–36

Terray P (1994) An evaluation of climatological data in the Indian Ocean area. J Met Soc Japan 72: 359–386

Todd PM, Wallace JM (2003) Recent trends in the Southern Oscillation Joint Institute for the Study of the Atmosphere and Ocean (JISAO). jisao.washington.edu/wallace/sotrends121803.pdf

Trenberth KE (1990) Recent observed interdecadal climate changes in the Northern Hemisphere. Bull Amer Meteor Soc 71: 988–993

Trenberth KE, Hoar TJ (1996) The 1990–1995 El Niño Southern Oscillation event: longest on record. Geophys Res Lett 23: 57–60

Vicente-Serrano SM (2005) Differences in spatial patterns of drought on different time scales: an analysis of the Iberian Peninsula. Water Resour Manag 20: 1

Walker ND (1990) Links between South African summer rainfall and temperature variability of the Agulhas and Benguela Currents systems. J Geophys Res 95: 3297–3319

Wang B (1995) Interdecadal changes in El Niño onset in the last four decades. J Climate 8: 267–285

Washington R, Swann M, New M (2003) Tropical oceans and the predictability of southern African rainfall in the HadCM3 coupled climate model. Cliva Exchanges 27: 2003

Waylen P, Henworth S (1996) A note on the timing of precipitation variability in Zimbabwe, as related to the Southern Oscillation. Int J Climatol 16: 1137–1148

Webster P, Moore JA, Saji NH, Goswami BN, Vinayachandran PN, Yamagata T (1999) A dipole mode in the tropical Indian Ocean. Nature 401: 360–363

World Bank (2006) Agriculture and rural development, regions, Sub Sahara Africa 2006

Yamagata T, Behera SK, Rao SA, Guan Z, Ashok K (2002) The Indian Ocean dipole: a physical entity – CLIVAR Exchanges, 2002

Yamagata T, Behera SK, Luo J, Masson S, Delecluse P, Gualdi P, Navarra A (2003) Impact of the Indian Ocean Dipole on the East African Short Rains: a CGCM study. CLIVAR Exchanges 27: 43–45

Authors' addresses: D. Manatsa (e-mail: dmanatsa@buse.ac.zw), W. Chingombe, H. Matsikwa, Faculty of Science, Bindura University of Science Education, P. Bag 1020, Bindura, Zimbabwe; C. H. Matarira, Department of Geography and Environmental Science, National University of Lesotho, Roma 180, Lesotho.